JOURNAL OF MAGNETIC RESONANCE **124,** 263–266 (1997)
ARTICLE NO. MN961055

Dynamic Nuclear Polarization Imaging in Very Low Magnetic Fields as a Noninvasive Technique for Oximetry

THIERRY GUIBERTEAU AND DANIEL GRUCKER

Institut de Physique Biologique, URA 1173 du CNRS, 4, rue Kirschléger, 67085 Strasbourg Cedex, France

Received October 29, 1996

Dioxygen is ubiquitous in energy metabolism. Its role is crucial in metabolic cycles as oxidative phosphorylation and is very important in radiotherapy efficiency. As such, it is very useful to develop a technique suitable for monitoring *in vivo* partial pressure of dioxygen (pO_2). Several techniques can provide accurate pO_2 measurements in cells and tissues, but cannot be performed on living animals. These include the Clark electrode (*1*), which allows measurements with an accuracy of 1.5 mm Hg. Phosphorescence quenching (*2*) also permits measurements of very low pO_2 (1.5×10^{-2} mm Hg), but is only suitable for surface measurements (less than 1 mm in depth). Noninvasive techniques, like nuclear magnetic resonance and electron paramagnetic resonance, seem to be the most suitable for *in vivo* measurements. ^{17}O NMR (*3–7*) has been used to study rat-brain oxygenation. The main drawback of this method, as in analogous positron emission tomography techniques, lies in the necessity of using isotopes.

One noninvasive technique, NMR spectroscopy of the proximal histidine NH in deoxymyoglobin (*8, 9*) has been demonstrated to reflect cellular deoxygenation, but has not allowed spatial localization of dioxygen content. ^{19}F magnetic resonance imaging (*10–13*) can also provide a measurement of pO_2 in tissues. The longitudinal relaxation rate of ^{19}F in perfluorochemicals has a linear relationship with pO_2, but high concentrations of the perfluorochemical solutions are necessary for *in vivo* applications. Echo-planar imaging can detect effects of O_2 on the NMR signal but the respective contributions of the oxygen concentration, flow effect, and susceptibility of deoxyhemoglobin remain controversial (*14–17*).

EPR with the use of free radicals as spin labels appears to be the most accurate technique for *in vivo* pO_2 measurements (*18–20*). In presence of O_2, EPR parameters of free radicals can change because of the paramagnetism of O_2. EPR oximetry can detect dissolved molecular oxygen concentrations as low as 10^{-7} *M*. Moreover, EPR imaging techniques allow spatial localization of dioxygen content, but *in vivo* experiments are limited to small animals. The nonresonant absorption of the electromagnetic waves used (0.7–9 GHz) and the dielectric losses due to water content can increase the temperature of the sample. Therefore, the future of *in vivo* EPR oximetry is dependent on the development of low-magnetic-field EPR spectroscopy to decrease the frequencies of the electromagnetic waves. Dynamic nuclear polarization (DNP), a well-known magnetic double-resonance technique (*21, 22*), can overcome many drawbacks associated with EPR. DNP permits a combination of the sensitivity of EPR in oximetry with the sensitivity of NMR to water protons. The aim of this Communication is to present DNP imaging in very low magnetic fields as a new noninvasive technique for *in vivo* oximetry, first by considering the sensitivity to dioxygen concentration of the Overhauser factor, then by analyzing the signal-to-noise ratio of the images obtained by DNP imaging in very low magnetic fields.

DNP effects can be observed with systems containing free radicals dissolved in a protonated solvent. When an EPR transition of a free radical is saturated by a radiofrequency field, the NMR signal of the solvent protons increases. This enhancement of the NMR signal is called the Overhauser factor (or DNP factor). In high magnetic fields, the theoretical Overhauser factor for a free radical with one unpaired electron is equal to −659 (the minus sign reflects a 180° phase change of the NMR signal), corresponding to the ratio of the magnetogyric ratios of the electron and the protons. This value is calculated assuming a pure scalar interaction between the electron and the solvent protons and a total electronic relaxation mechanism by the electron–proton interaction (*23*). As in EPR experiments, the Overhauser factor is dependent on the pO_2 of the sample. The sensitivity of DNP imaging has been demonstrated on free-radical solutions (*24, 25*) and on perfused hearts (*26*). The effect of O_2 on the DNP factor has been studied quantitatively in high magnetic fields using nitroxides dissolved in water (*27*). Nitroxides are free radicals with one unpaired electron coupled by a scalar interaction, also called contact interaction, to a nitrogen nucleus (spin 1 for ^{14}N or spin $\frac{1}{2}$ for ^{15}N). This interaction induces a hyperfine splitting of the energy levels given by the Breit–Rabi equation (*28*). Ten EPR transitions

1090-7807/97 $25.00

can be induced for a ^{14}N nitroxide in low magnetic fields. Eight π transitions are induced with a radiofreqency field perpendicular to the main magnetic field, and two σ transitions are induced with a radiofrequency field parallel to the main magnetic field. In high magnetic fields, only 3 π EPR transitions are allowed, giving the classical EPR spectrum of nitroxide with three lines. In low magnetic fields, the field seen by the unpaired electron is not the applied field, but the magnetic field due to the nitrogen nucleus. Therefore, the NMR signal of the water proton coupled to the unpaired electron can be enhanced by a DNP factor of approximately -2000 compared to the equilibrium NMR signal in the main magnetic field.

DNP experiments were performed at room temperature with 140 ml buffered phosphate solution (pH 7.4) of 3 m*M* TXO nitroxide (4-oxo-2,2,6,6-tetramethyl-piperidinyl-^{14}N-oxyl) from Aldrich. Dioxygen concentration of samples was determined after calibration of a mass flow controller (FC 280A from Teflinox, Wasselonne, France). Details of the DNP spectrometer and of the DNP imager were described previously (*29*). Measurement of the sensitivity to dioxygen of the Overhauser factor was done by field-cycling dynamic nuclear polarization (FCDNP). The signal-acquisition sequence was composed by an EPR irradiation (1.5 s duration) followed by a 90° NMR pulse (3 s repetition time, four accumulations). In the FCDNP experiment, the magnetic field is switched to different values for the duration of the EPR irradiation, then is switched to 68 G in less than 5 ms for the NMR signal detection. DNP images (128 × 128 pixels) were obtained by a one-slice multiecho NMR (20 mm slice thickness, 20 echoes summation, 1.5 s duration for the EPR irradiation, 3 s repetition time, and four accumulations). Total acquisition time was 17 mn. The field-cycling dynamic nuclear polarization technique was used for experiments performed at 0.5 and 3.4 G. EPR irradiation was performed at 198, 74, and 69 MHz respectively with a 68, 3.4, and 0.5 G magnetic field respectively.

The dependence of the Overhauser factor versus the dioxygen concentration in three different magnetic fields is shown in Fig. 1. The Breit–Rabit equation shows that the paramagnetic energy diagram for a ^{14}N nitroxide (spin 1) is composed of six levels. The levels are usually classed by decreasing energy order (E_1 for the highest level, E_6 for the lowest level). A T_{ij} EPR transition is a transition induced between the levels i and j. Preliminary results (*29, 30*) showed that of the 10 allowed EPR transitions of a nitroxide in a low magnetic field, only 6 give a NMR enhancement suitable for DNP imaging and the T_{16} transition gives the largest NMR enhancement. Therefore experiments at 0.5 and 3.4 G were performed with irradiation of T_{16} transition. Results at 68 G with irradiation of the T_{25} transition are presented as a reference of classical high field experiments. The theoretical Overhauser factors (-110 in high magnetic field, -2000 in low magnetic field) are not reached, because the electronic relaxation mechanism by the proton–electron

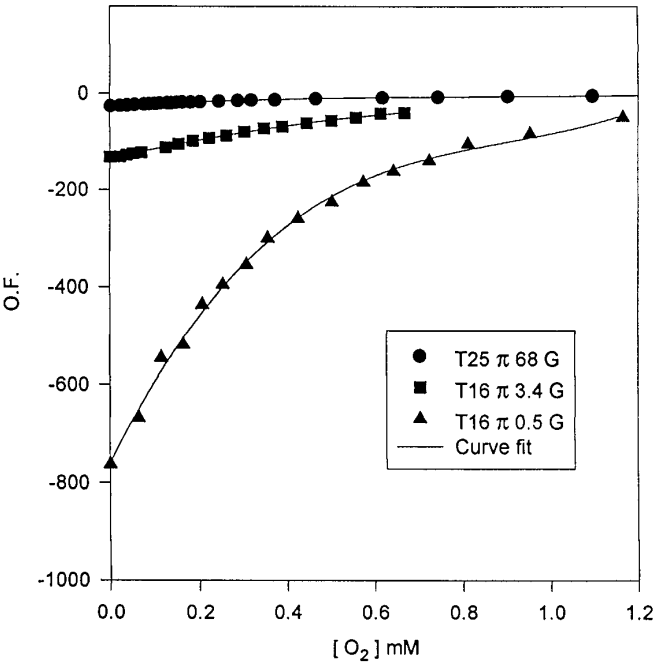

FIG. 1. The Overhauser factor versus the dioxygen concentration. The curve with the T_{25} EPR transition (●) is presented as a reference in high magnetic fields without field cycling. For the T_{16} transition, the EPR irradiation was performed at 3.4 G (■) with a 74 MHz radiofrequency field and at 0.5 G (▲) with a 69 MHz radiofrequency field.

interaction and the dipolar coupling between protons and electrons is only partial for TXO nitroxide in water (*31*). The absolute value of the Overhauser factor and its sensitivity to oxygen are larger when the magnetic field is lower. The best sensitivity to oxygen is achieved for an EPR saturation at 0.5 G and for dioxygen concentrations between 0 and 0.4 m*M*, which correspond to the *in vivo* molecular oxygen concentrations. For this concentration range, the calculated sensitivity of the Overhauser factor to dioxygen (ΔO.F./$\Delta[O_2]$ in mmol^{-1}) is approximately equal to 1230 at 0.5 G, 63 at 3.4 G, and 20 at 68 G respectively.

In DNP, as in NMR imaging, the signal-to-noise ratio is the main parameter for the quality of the image. For imaging, a signal-to-noise ratio higher than 10 is required. Images of seven tubes filled with a 3 m*M* TXO solution are presented in Fig. 2. The concentration of dioxygen of the different tubes varies from 0 to 1 m*M*. The figure shows the feasibility to perform DNP imaging in very low magnetic fields.

In order to compare the images, we calculated the signal-to-noise ratio (S/N). The average intensity was calculated by defining a region of interest (ROI) centered on the cross section of each tube. The noise was calculated as the mean intensity of a ROI outside of the tubes. The effects of dioxygen concentration on the signal-to-noise ratio are shown in Fig. 3. To compare the results with those obtained in high magnetic fields, we have measured the signal-to-noise ratio of the NMR signal while the T_{25} EPR transition was saturated in a 68 G

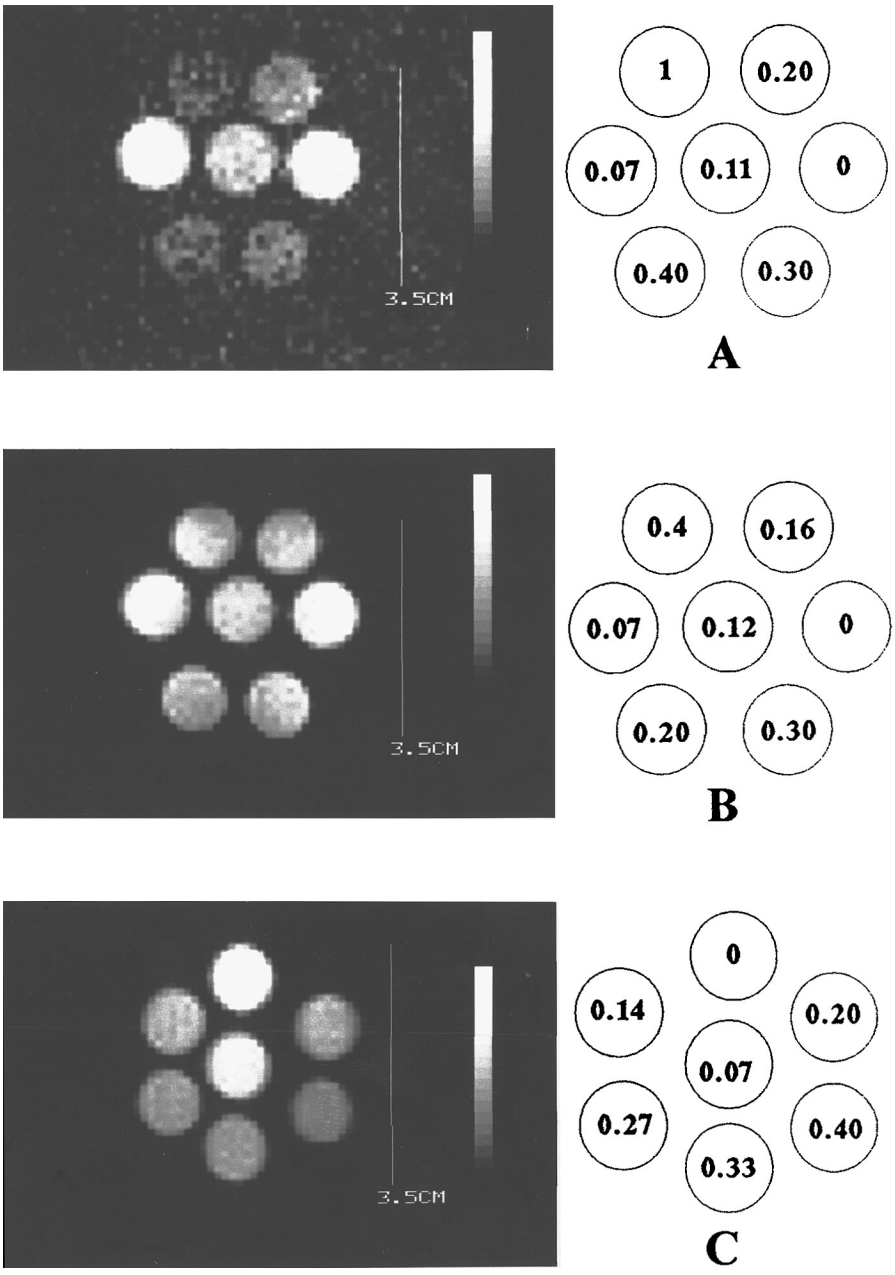

FIG. 2. DNP imaging of TXO tubes with different dioxygen concentrations. The magnetic field strength was 0.5, (A), 3.4, (B), and 68 G (C). Dioxygen concentration (in mM) of tubes is presented beside the images.

magnetic field with a 198 MHz radiofrequency field. This measurement was performed without field cycling. The T_{25} transition is used in the classical oximetry experiments by EPR. The signal-to-noise ratio is larger when the magnetic field is higher but, as shown in Fig. 1, the sensitivity to oxygen is better when the magnetic field is lower. Therefore on one hand, the Overhauser factor is larger for experiments at 0.5 G than at 3.4 G, while on the other hand, the signal-to-noise ratio is smaller, due to the NMR noise which is more sensitive to the thermal noise and to magnetic pollution of the environment at 0.5 G than at 3.4 G.

Although the signal-to-noise ratio of the image at 68 G with a 198 MHz radiofrequency field is larger by a factor of 1.8 over that of the image at 3.4 G with a 74 MHz radiofrequency field, the power deposition, which is roughly proportional to the square of the frequency, is reduced approximately sixfold. This explains why DNP images performed at 68 G with a 198 MHz radiofrequency field induced an increase of sample temperature of 4°C. Such a DNP experiment cannot be performed *in vivo.* No temperature increase was detected at 3.4 G with a 74 MHz radiofrequency field. Therefore, *in vivo* application of DNP requires a radio-

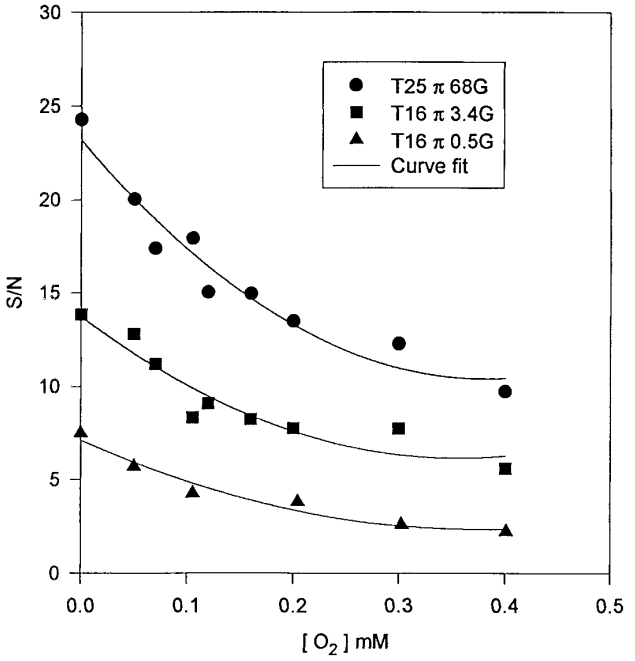

FIG. 3. Signal-to-noise ratio (S/N) versus the dioxygen concentration. The S/N ratio was calculated by performing images of tubes with different dioxygen concentrations.

frequency field lower than 100 MHz in order to avoid prohibitive increases in temperature. The use of free radicals with hyperfine coupling like nitroxides allows a decrease of the radiofrequency field to about 75 MHz in very weak magnetic fields. In such magnetic fields, sensitivity of DNP to oximetry is larger than that in high magnetic fields. The future of oximetry by DNP imaging requires the development of new nitroxides with a better stability in biological fluids. The optimization of acquisition devices will surely increase the quality of the NMR images obtained at such a low magnetic field.

ACKNOWLEDGMENTS

The authors thank Ms. Corinne Marrer for her skilled technical assistance and Dr. Ohlenbush for helpful discussions. T.G. has benefited from a postdoctoral grant from the Société de Secours des Amis des Sciences. Mr. Loewenguth and Mr. Ringeisen from Bruker Spectrospin (Wissembourg, France) are fully thanked for the design of the DNP probes.

REFERENCES

1. L. C. Clark, *Am. Soc. Artif. Intern. Organs* **2,** 41 (1956).
2. J. M. Vanderkooi, G. Maniara, T. J. Green, and D. F. Wilson, *J. Biol. Chem.* **262,** 5476 (1987).
3. J. Pekar, L. Ligeti, Z. Ruttner, R. C. Lyon, T. M. Sinnwell, P. Van Gelderen, D. Fiat, C. T. Moonen, and A. C. McLaughlin, *Magn. Reson. Med.* **21,** 313 (1991).
4. G. D. Mateescu, J. C. LaManna, W. D. Lust, L. M. Mars, and J. Tseng, Abstracts of the Society of Magnetic Resonance in Medicine, 10th Annual Meeting, San Francisco, p. 1031, 1991.
5. G. D. Mateescu and D. Fercu, Abstracts of the Society of Magnetic Resonance in Medicine, 12th Annual Meeting, New York, p. 110, 1993.
6. I. Ronen and G. Navon, *Magn. Reson. Med.* **32,** 789 (1994).
7. R. Reddy, A. H. Stolpen, and J. S. Leigh, *J. Magn. Reson. B* **108,** 276 (1995).
8. U. Kreutzer, Y. Chung, D. Butler, and T. Jue, *Biochim. Biophys. Acta* **1161,** 33 (1993).
9. Z. Wang, E. A. Noyszewski, and J. S. Leigh Jr., *Magn. Reson. Med.* **14,** 562 (1990).
10. F. Girard, P. Poulet, J. Steibel, and J. Chambron, *NMR Biomed.* **6,** 366 (1993).
11. R. P. Mason, F. M. H. Jeffrey, C. R. Malloy, E. E. Babcock, and P. P. Antich, *Magn. Reson. Med.* **27,** 310 (1992).
12. H. P. Shukla, R. P. Mason, D. E. Woessner, and P. P. Antich, *J. Magn. Reson. B* **106,** 131 (1995).
13. U. Nöth, R. Deichmann, H. Adolf, C. Schwarzbauer, and A. Haase, *J. Magn. Reson. B* **105,** 233 (1994).
14. B. E. Hoppel, R. M. Weisskoff, K. R. Thulborn, J. B. Moore, K. K. Kwong, and B. R. Rosen, *Magn. Reson. Med.* **30,** 715 (1993).
15. R. Turner, P. Jezzard, H. Wen, K. K. Kwong, D. Le Bihan, T. Zeffiro, and R. S. Balaban, *Magn. Reson. Med.* **29,** 277 (1993).
16. R. S. Menon, S. Ogawa, D. W. Tank, and K. Ugurbil, *Magn. Reson. Med.* **30,** 380 (1993).
17. P. A. Bandettini, A. Jesmanowicz, E. C. Wong, and J. S. Hyde, *Magn. Reson. Med.* **30,** 161 (1993).
18. J. S. Hyde, and W. K. Subczynski, *in* ''Biological Magnetic Resonance'' (L. J. Berliner and J. Reuben, Eds.), p. 399, Plenum Press, New York, 1989.
19. J. L. Zweier, M. Chzhan, U. Ewert, G. Schneider, and P. Kuppusamy, *J. Magn. Reson. B* **105,** 52 (1994).
20. A. I. Smirnov, R. B. Clarkson, and R. L. Belford, *J. Magn. Reson. B* **111,** 149 (1996).
21. A. Abragam, ''The Principles of Nuclear Magnetism,'' Clarendon Press, Oxford, 1961.
22. R. D. Bates, *Magn. Reson. Rev.* **16,** 237 (1993).
23. W. Müller-Warmuth and K. Meise-Gresch, *Adv. Magn. Reson.* **11,** 1 (1983).
24. D. Grucker and J. Chambron, *Phys. Med.* **5,** 329 (1989).
25. D. Grucker, *in* ''Magnetic Resonance Spectroscopy'' (B. Blümich, W. Khun, Eds.), p. 573, VCH, Weinheim, 1992.
26. D. Grucker and J. Chambron, *Magn. Reson. Imaging* **11,** 691 (1993).
27. D. Grucker, T. Guiberteau, and B. Eclancher, *Magn. Reson. Med.* **34,** 219 (1995).
28. G. Breit and I. I. Rabi, *Phys. Rev.* **38,** 2082 (1931).
29. T. Guiberteau and D. Grucker, *J. Magn. Reson. B* **110,** 47 (1996).
30. G. Planinsic, T. Guiberteau, and D. Grucker, *J. Magn. Reson. B* **110,** 205 (1996).
31. D. Grucker, T. Guiberteau, B. Eclancher, J. Chambron, R. Chiarelli, A. Rassat, G. Subra, and B. Gallez, *J. Magn. Reson. B* **106,** 101 (1995).